JOURNAL OF MATERIALS SCIENCE **36** (2001) 1301 – 1306

Application of an ultrasonic technique to creep cavitation in silicon nitride

J. W. CAO
Japan Fine Ceramics Center, Nagoya, 456-8587 Japan

F. LOFAJ
Institute of Materials Research of the Slovak Academy of Sciences, 043 53 Kosice, Slovakia

A. OKADA
Japan Fine Ceramics Center, Nagoya, 456-8587 Japan
E-mail: okada@jfcc.or.jp

A non-destructive method based on measurements of ultrasonic wave velocities and Young's modulus is proposed for quantification of creep cavitation in silicon nitride. Tensile creep tests of silicon nitride were conducted at 1400°C in air and the tests were periodically interrupted to measure the longitudinal and transverse ultrasonic wave velocities and Young's modulus. The velocities and Young's modulus decreased linearly with tensile creep strain. The volume fraction of cavities was estimated from the values of the ultrasonic wave velocities and Young's modulus, and compared with the cavity volume predicted from tensile creep strain. The dependence of Young's modulus on volume fraction of cavities is discussed.

1. Introduction

Silicon nitride is a prime candidate for structural components used at elevated temperatures in applications such as advanced gas turbines with higher efficiency and lower pollutant emission levels [1, 2]. One of the principal limitations for such applications is, however, reliable prediction of their lifetime. Failure at elevated temperatures usually occurs via subcritical crack growth or creep rupture mechanisms [3]. In the former case, time-to-failure is predicted from the crack velocity and inert strength. In the latter case, the lifetime is often predicted using empirical relationships describing creep rupture [4–7]. For example, the Larson-Miller method [8] predicts the lifetime based on the data obtained at different stresses and temperatures, and the creep rupture prediction using the Monkman-Grant relation [9] is based on the minimum strain rates. Another method to estimate the lifetime is to use a stress-rupture diagram. However, the conditions in the actual applications are not constant and measuring strains on turbine rotors during operation is unrealistic. In addition, a nonlinear relationship between stress and time-to-failure has been observed in creep rupture diagrams in silicon nitrides at high temperatures [6, 7]. In this case, the prediction of long-term lifetime based on a limited number of short-term tests is ambiguous. This indicates that better understanding of the underlying physical processes occurring during deformation is necessary to ensure the reliability of the lifetime prediction.

It is well known that creep deformation in ceramics can occur by several mechanisms such as diffusion, viscous flow and solution-precipitation, and that creep rupture is related to the accumulation of cavities. However, the major deformation mechanism during tensile creep in vitreous-bonded silicon nitride is also cavitation [10–19]. Lofaj *et al*. suggested that cavitation fully contributes to tensile strain and found that cavitation strain produces more than 90% of the total elongation [13]. Creep asymmetry, which is typical for vitreous-bonded ceramics, is a consequence of different contribution of cavities to tensile and compressive creep strain [13]. A recent creep model by Luecke and Wiederhorn [14], which is based on the cavitation mechanism, explains an exponential increase in creep rates at high stresses. Predictions by this model agree with the creep data in different grades of silicon nitrides [17–19]. Since the model implies that cavitation is the dominant tensile creep mechanism in silicon nitride and similar granular materials, monitoring the density of cavities would provide important information about creep damage accumulation and eventually contribute to the development of a more reliable life prediction method.

Because cavitation is equivalent to porosity in terms of density change, changes in density-sensitive parameters, such as ultrasonic wave velocity and Young's modulus, should be an effective means for quantifying the evolution of cavitation. The objective of the present paper is to explore the possibility of a nondestructive ultrasonic wave velocity method to characterize the creep damage evolution in silicon nitride.

2. Experimental procedure

Commercially available self-reinforced silicon nitride designated as SN88M (NGK Insulators, Ltd., Nagoya,

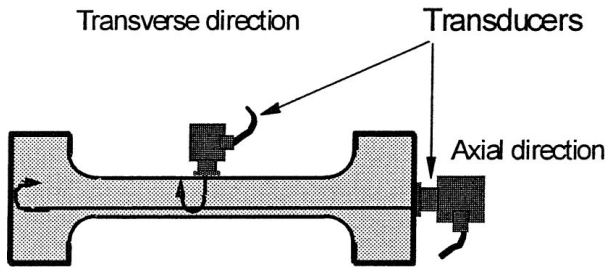

Figure 1 Geometry of a specimen used in the interrupted tensile creep test. Ultrasonic wave velocity was measured in the axial direction (along the specimen length) and across the width of the gage.

Japan) was used in the present study. The microstructure of this material has a typical bimodal grain size distribution with a small number of large elongated grains of β- Si_3N_4 (diameter 5–10 μm, length 50–80 μm) randomly distributed in a fine grained (diameter 0.5–0.8 μm) β- Si_3N_4 matrix.

Fig. 1 shows a dog-bone specimen used for tensile creep tests. The gage length of the specimen is 40 mm and it has a rectangular cross section of 4.0 mm $\times$ 6.0 mm. Creep experiments were conducted in HT 300 testing machines (Toshin Industrial Co., Ltd., Tokyo, Japan) with a lever arm, dead weight loading system and hot grips with four pins. Creep deformation was measured with two linear variable differential transducers (LVDT) located outside of the furnace. The tests were carried out in air at 1400°C under a tensile stress of 140 MPa and periodically interrupted after 30 h or 40 h.

The velocities of the longitudinal and transverse ultrasonic waves were measured using a pulse-echo technique with a pulser/receiver operating at 200 MHz (Model 5900 PR, Panametrics). Magnetostrictive transducers of 20 MHz and 10 MHz were used for measuring the velocities of the longitudinal and transverse waves, respectively. Silicon oil and water based couplings were used between the specimen and the corresponding transducer. Using a digital oscilloscope, time intervals between the echoes of the primary signal were measured. The measurements were conducted in the directions parallel and perpendicular to tensile loads for the as-received specimen and after each increment of strain. The former corresponds to the direction along the gage length and the latter to the direction across the width of the specimen (see Fig. 1). The velocities of both types of ultrasonic waves were calculated from the time intervals and corresponding length ($\sim$70 mm) and width (6 mm) of the specimen measured with a digital micrometer with an accuracy of ± 2 μm.

Young's moduli were measured at room temperature using four or eight strain gages and gradual loading up to 140 MPa in the as-received state and after each interruption. Strain gages were glued on each face of the specimen at the middle or both ends of the gage (see Fig. 1). This procedure was simultaneously used for control of alignment and adjustment of the loading train.

3. Results and discussion

Fig. 2 shows a creep curve characterizing the tensile creep behavior of SN88M at 1400°C in air under

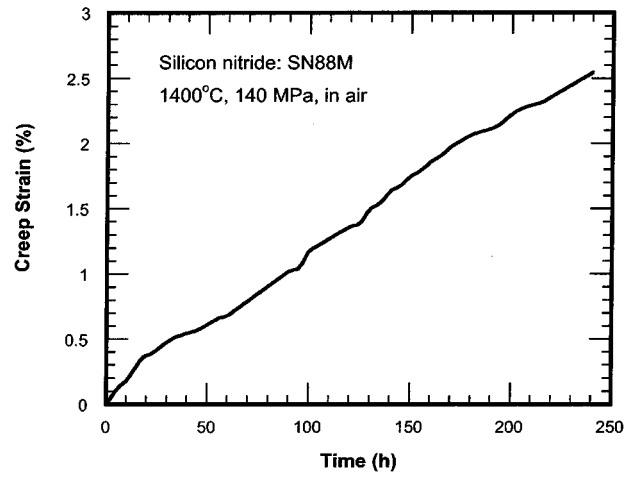

Figure 2 Tensile creep curve of SN 88M at 1400°C in air under a tensile stress of 140 MPa.

a stress of 140 MPa. After loading, the creep strain gradually increases approximately at a creep rate of 2.8×10^{-8} s^{-1} after exhibiting a transient creep region of initial 20 hours. The stress dependence of the creep rates and lifetime as well as the details of the creep damage were described elsewhere [7, 12, 13, 15, 16, 18–20].

Fig. 3a and b show the relative ultrasonic wave velocity changes in longitudinal and transverse waves as a function of creep time in the axial direction parallel to the stress. The relative ultrasonic wave velocity change may be defined as

$$\frac{\Delta v}{v_0} = \frac{(v_0 - v)}{v_0}$$

where v_0 is an initial ultrasonic wave velocity measured before the creep test and used as a reference. This corresponds to the as-received (cavity-free) specimen. The relative ultrasonic velocities both in longitudinal and transverse waves decrease with creep time. In Fig. 3c and d, the relative velocity changes in the transverse direction perpendicular to the stress are shown. The ultrasonic wave velocities similarly decrease with creep time or strain. Note that the decrease in the velocity of the longitudinal wave is more significant than that of the transverse wave and that the relative changes in the velocity values are smaller in the axial direction than across the width of the specimen. In addition, the scatter in the data measured in the axial direction is greater. The corresponding reliability factors of the least square fits are also smaller in the axial direction despite greater relative errors in the length measurements. This seems to result from the fact that the data in the axial direction are an average of the velocities in the gage and two gripping parts, which are more dense, whereas the data obtained in the transverse direction correspond only to the velocities in the gage section. As a result, the transverse direction is preferable with regard to the specimen's properties and reliability of the data and the velocity measurement of the longitudinal wave is slightly more effective than that of the transverse waves.

Fig. 4 shows the changes in Young's modulus during the creep test. The values were calculated from

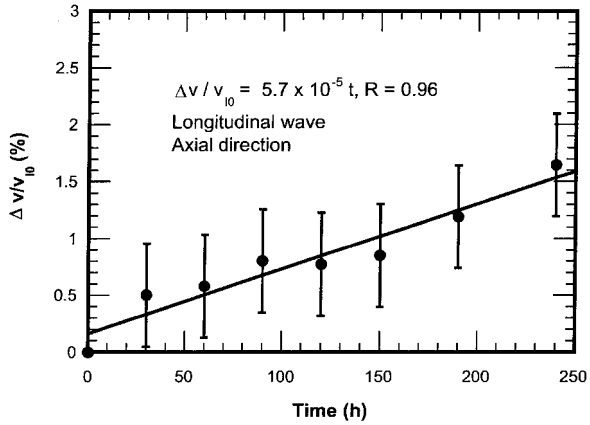

(a)

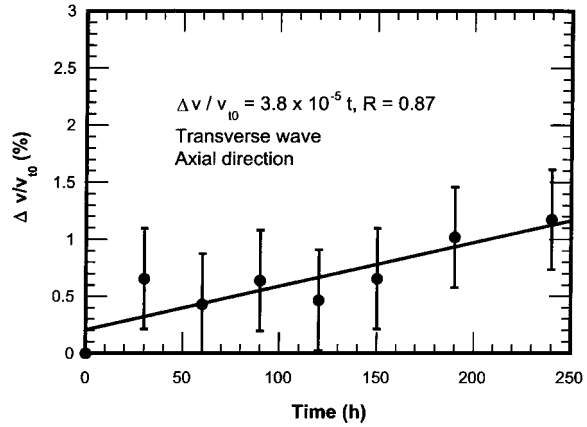

(b)

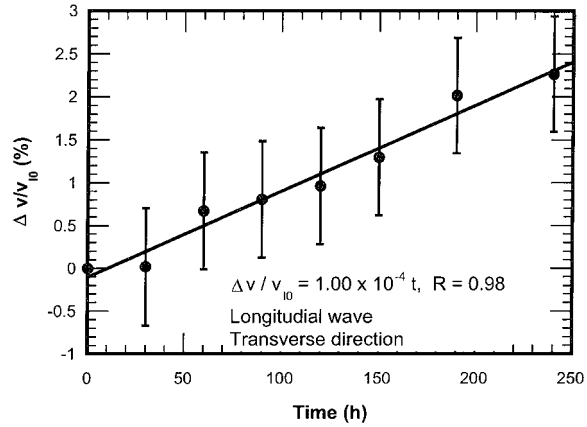

(c)

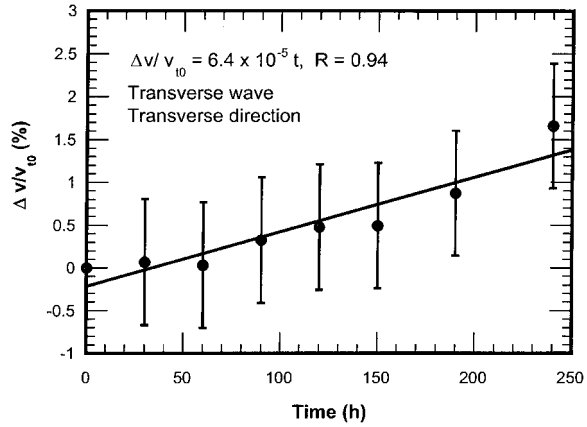

(d)

Figure 3 Dependence of the relative ultrasonic velocity change on creep strain: (a) the longitudinal wave velocity in the axial direction, (b) the traverse wave velocity in the axial direction, (c) the longitudinal wave velocity across the width of the gage and (d) the traverse wave velocity across the width of the gage.

TABLE I Summary of ultrasonic wave velocity and Young's modulus changes during tensile creep in SN88M silicon nitride

Creep time (h)	Creep strain (%)	v_l (m/s)	v_t (m/s)	E (GPa)
0	0.00	10412 (10320)	5840 (5791)	294 ± 10
30	0.48	10410 (10268)	5836 (5753)	292 ± 9
60	0.68	10342 (10260)	5838 (5766)	—
90	1.02	10328 (10237)	5821 (5754)	289 ± 19
120	1.36	10312 (10240)	5812 (5764)	283 ± 12
150	1.75	10277 (10232)	5811 (5753)	—
190	2.11	10202 (10197)	5789 (5732)	280 ± 24
240	2.55	10176 (10150)	5743 (5723)	279 ± 17

*The ultrasonic wave velocities shown here were measured across the width of the specimen. The values in the axial direction are shown in brackets.

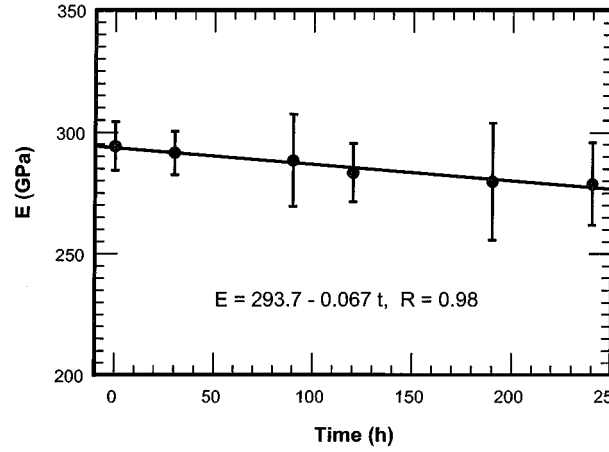

Figure 4 Time dependence of Young's modulus during interrupted creep tests obtained from the stress-strain data from strain gages during loading at room temperature.

strain gage data taken during interrupted tests. The initial value of Young's modulus in the specimen prior to testing is 295 ± 10 GPa. The value decreases gradually with creep damage and reaches 279 ± 17 GPa when a strain of 3.17% has been accumulated after creep for 240 hours.

Table I summarizes creep strain, Young's modulus and the corresponding ultrasonic wave velocity data. The values of ultrasonic wave velocities in the transverse direction are also listed and the values corresponding to the axial direction are given in brackets. This is because the velocity measurements are more reliable when they are conducted in the transverse direction.

It is well known that Young's modulus may be determined from ultrasonic wave velocities and the density of the material. The density, ρ, may be defined as [21]

$$\rho = E\left(v_l^2 - v_t^2\right) / \left(3v_l^2\, v_t^2 - 4v_t^4\right) \qquad (1)$$

where E is Young's modulus, and v_l and v_t are the velocities of the longitudinal and transverse waves, respectively. This equation enables us to calculate the density corresponding to each increment of creep strain when Young's modulus and ultrasonic wave velocities are known.

According to the cavitation creep model, the relative change in density during creep, $(\rho_0 - \rho)/\rho_0$, is equal to the volume fraction of cavities, f_v,

$$f_v = \frac{(\rho_0 - \rho)}{\rho_0} \quad (2)$$

where ρ_0 is the density of the material prior to testing. Note that the volume fraction of cavities is somewhat smaller than the porosity because this expression ignores the influence of the initial porosity in the as-received material and possible changes in the microstructure due to heat treatment. Using the ultrasonic wave velocity and Young's modulus data (see Table I), the volume fraction of cavities is calculated according to Equation 2 and plotted as a function of strain in Fig. 5. Lofaj *et al*. proposed another method to estimate the volume fraction of cavities in this grade of silicon nitride, based on a linear relationship existing between the volume fraction of cavities and tensile strain, ε, [13]

$$f_v = k\varepsilon \quad (3)$$

where k is the coefficient of proportionality. Values of k are in the range 0.92 to 0.95 and this suggests that cavitation is responsible for more than 90% of tensile strain [13]. Thus, the volume fraction of cavities can be simply estimated from the axial strain. Fig. 5 shows the volume fraction of cavities calculated from Equation 2, assuming $k = 0.90$. It can be seen that the two functions overlap in spite of the relatively large scatter in the ultrasonic wave velocity based data. This gives additional confirmation that the cavitation mechanism is responsible for creep deformation. It should be noted that the large scatter in f_v using ultrasonic wave velocity based data is due to accumulated errors in calculating the density in accordance with Equation 1.

Fig. 6a and b show the dependence of the relative velocities of the longitudinal and transverse waves, calculated from the measurements in the transverse direction, on the volume fraction of cavities according to Equation 3. It is seen that ultrasonic wave velocities decrease linearly with the volume fraction of cavities. The corresponding coefficients of proportionality for

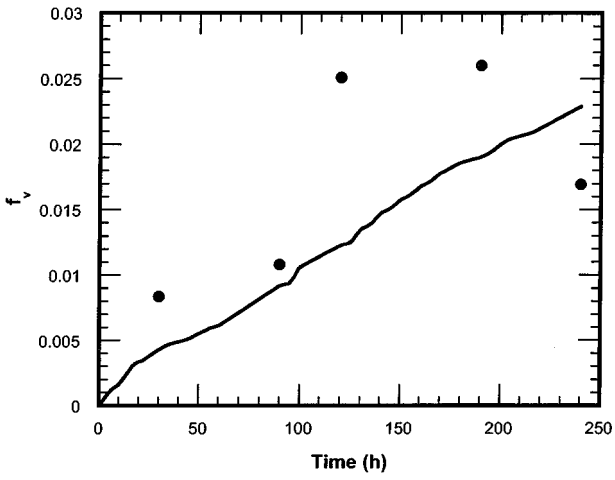

Figure 5 A comparison of the volume fraction of cavities during creep in silicon nitride calculated according to Equations 2 and 3. Closed circles denote the values calculated from Equation 2 and the solid line indicates the values calculated from Equation 3.

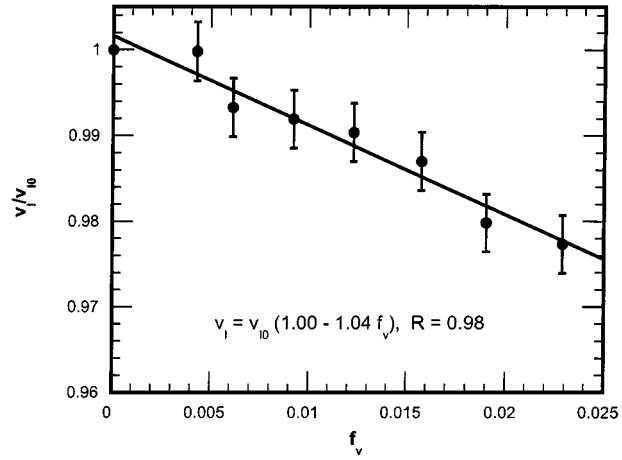

(a)

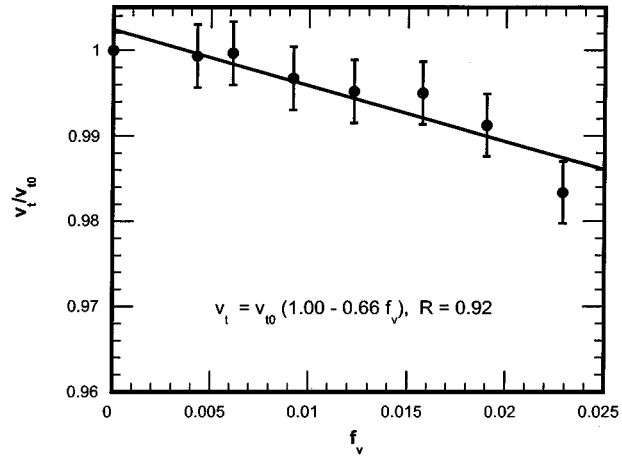

(b)

Figure 6 The relationship between volume fraction of cavities and ultrasonic velocity of (a) longitudinal waves and (b) transverse waves.

the longitudinal and transverse waves are 1.04 and 0.66, respectively. The higher coefficient for the longitudinal waves indicates that the longitudinal waves are slightly more effective than transverse waves for monitoring creep damage during tensile creep.

The physical meaning of the decrease in ultrasonic wave velocities of porous solids is usually described in terms of the interaction of the ultrasonic wave front with the pores. Therefore, the wave velocity of a porous body is analyzed, based on the concept of ultrasonic waves propagating around the pore. Hurst *et al*. analyzed the velocity of ultrasonic wave propagating along a cylindrical hole and reported that the velocity decreases with a decrease in the radius of the hole [22]. Ying [23] measured the velocities around a cylindrical hole in a glass plate and reported that the relative velocities of the longitudinal and transverse waves to a fully dense solid are 0.96 and 0.86, respectively. Based on an analysis incorporating the arrival probabilities of ultrasonic waves, Takatsubo *et al*. expanded on this idea and proposed a model in which the incident wave interacts with the pore and is deflected around the pore surface [24]. This causes a delay in the propagation time, and the velocity of the longitudinal waves, v_l, is given by [24]

$$\frac{v_l}{v_{l0}} = \{1 + 3p(\pi s/q - 2)/8\}^{-1},$$

where p is porosity, $q = v_c/v_p$, $s = l_p/(2\pi r)$, v_c is the effective ultrasonic wave velocity around the pore, v_{l0}

is the velocity of the longitudinal wave in a fully dense solid, r is the radius of the pore, and l_p is the circumference of the pore. In the case of low porosity, this relationship may be simplified to

$$\frac{v_l}{v_{l0}} = 1 - cp \tag{4}$$

The value of the coefficient c can be determined from the original relationship for longitudinal waves. In the case of spherical voids and ratio $v_c/v_{l0} = 0.96$ [23], the theoretical value of c is approximately 0.48. This is considerably smaller than the value measured in the current work. A comparison with the literature data also indicates even larger differences compared with the theoretical value. For example, Panakkal [25] analyzed the ultrasonic velocity data of sintered uranium dioxide in the pore volume fraction range of 0–0.28 and reported $c = 1.35$. Kumar *et al.* [26] summarized the c values from previous work and reported $c = 0.75$ for alumina and $c = 0.83$ for α-SiC. This is possibly because the theory assumes only spherical cavities in two dimensions while the experimental values reflect a large variety of pore shapes and distributions.

It is well known that Young's modulus also decreases with an increase in porosity. This dependence has been investigated over wide range of porosity by numerous authors and several types of relationships have been proposed [27–31]. However, for a porosity (or volume fraction of cavities) below 3%, all the relationships can be simplified to a linear dependence. As a result, the porosity dependence of Young's modulus within the range of porosity studied can be described as

$$\frac{E}{E_0} = 1 - bp \tag{5}$$

where E_0 is Young's modulus of a pore-free material and b is a coefficient describing the porosity dependence.

Fig. 7 shows the dependence of Young's modulus on the volume fraction of cavities, according to Equation 3. The data follow a linear relationship in agreement with Equation 5 and least square fitting leads to $b = 2.44$,

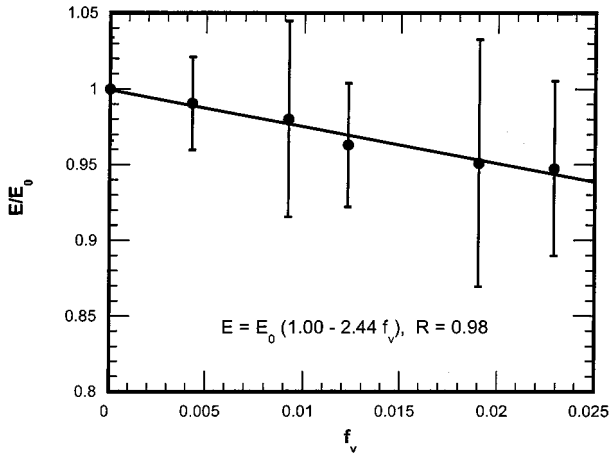

Figure 7 Dependence of Young's modulus on the volume fraction of cavities.

where p is replaced by f_v in the expression. This coefficient is consistent with the earlier data obtained in different silicon nitride ceramics [27, 28]. For example, Phani *et al*. [27] reported $b = 1.74$ for sintered silicon nitrides with porosity in the range of 0 to 26%. Datta *et al*. [28], who analyzed 156 sets of literature data and their own experiments on silicon nitride, reported coefficients in the range of 2.00 to 3.03 for porosities up to 38%. In addition, Fate investigated the density dependence of the shear modulus in silicon nitride by a similar pulse echo technique and obtained a value of b close to 2.0 [29].

The degradation of Young's modulus and ultrasonic wave velocity reduction obtained in current work on a limited number of specimens during creep provide similar coefficients to considerably larger sets of data from sintered materials. This emphasizes the importance of the ultrasonic wave velocity technique because it is a highly sensitive and very simple method for reliable and nondestructive detection of cavity accumulation during creep in silicon nitride ceramics.

4. Summary

The ultrasonic wave velocity technique was proven to be a suitable technique for the study and evaluation of cavitation during tensile creep in silicon nitride. Measurements of the velocities of the longitudinal and transverse ultrasonic waves were conducted during interrupted creep tests by a pulse-echo technique and it was revealed that their linear decrease is proportional to the strain and volume fraction of cavities. A combination of these data with independent measurements of Young's modulus confirmed the close correlation between tensile strain and the volume fraction of cavities and revealed that cavities are fully responsible for tensile strain in silicon nitride ceramics.

Acknowledgments

This work was funded by the New Energy and Industrial Technology Department Organization (NEDO) Project "Research and Development of Ceramic Gas Turbines (300 kW class)". The support for two of the authors (JWC and FL) provided by the Science and Technology Agency of Japan is highly appreciated. The authors are very grateful for helpful discussions with Y. Ikeda and H. Kawamoto and for the technical assistance with the ultrasonic wave velocity measurements by Y. Mizuta.

References

1. T. KAMEI and M. NISHIO, in Proceedings of the 1995 Yokohama International Gas Turbine Congress, vol. I, The 1995 Yokohama International Gas Turbine Congress Organizing Committee (Tokyo, Japan, 1995) p. 143.
2. T. NAKASHIMA, T. TATSUMI, I. TAKEHARA, Y. ICHIKAWA and H. KOBAYASHI, in Proceedings of 6th International Symposium on Ceramic Materials and Components for Engine, edited by K. Niihara, S. Kanzaki, K. Komeya, S. Hirano and K. Morinaga (Technoplaza Co., Ltd., Tokyo, Japan, 1998) p. 233.
3. G. D. QUINN, *J. Mater. Sci.* **25** (1990) 4361.
4. R. KOSSOWSKY, D. G. MILLER and E. S. DIAZ, *ibid.* **10** (1975) 983.

5. J.-L DING, K. C. LIU, K. L. MORE and C. R. BRINKMAN, *J. Amer. Ceram. Soc.* **77** (1994) 867.
6. M. N. MENON, H. T. FANG, D. C. WU, M. G. JENKINS and M. K. FERBER, *ibid.* **77** (1994) 1235.
7. Y. TAKIGAWA, J.-W. CAO, Y. IKEDA and H. KAWAMOTO, *Key Engineering Materials* **171–174** (2000) 841.
8. F. R. LARSON and J. MILLER, *Trans. ASME* **74** (1952) 765.
9. F. C. MONKMAN and N. J. GRANT, *Proc. Am. Soc. Test. Mater.* **56** (1956) 593.
10. M. K. FERBER, M. G. JENKINS, T. A. NOLAN and R. L YECKLEY, *J. Amer. Ceram. Soc.* **77** (1994) 657.
11. W. E. LUECKE, S. M. WIEDERHORN, B. J. HOCKEY, R. E. KRAUSE JR. and G. G. LONG, *ibid.* **78** (1995) 2085.
12. F. LOFAJ, A. OKADA, H. USAMI and H. KAWAMOTO, in Ceramic Transactions vol. 71 (Mass and Charge Transport in Ceramics), edited by K. Koumoto, L. M. Sheppard and H. Matsubara (The American Ceramic Society, Westerville, OH, 1997) p. 585.
13. F. LOFAJ, A. OKADA and H. KAWAMOTO, *J. Amer. Ceram. Soc.* **80** (1997) 1619.
14. W. E. LUECKE and S. M. WIEDERHORN, *ibid.* **82** (1999) 2769.
15. F. LOFAJ, J.-W. CAO, A. OKADA and H. KAWAMOTO, in Proceedings of 6th International Symposium on Ceramic Materials and Components for Engines, edited by K. Niihara, S. Kanzaki, K. Komeya, S. Hirano and K. Morinaga. (Technoplaza Co., Ltd., Tokyo, Japan, 1998) p. 713.
16. F. LOFAJ, H. USAMI, A. OKADA and H. KAWAMOTO, in "Engineering Ceramics '96: Higher Reliability Through Processing," edited by C. N. Babini, M. Haviar and P. Sajgalik (Kluwer Academic Publishers, Dordrecht, The Netherlands, 1997) p. 337.
17. R. E. KRAUSE, JR., W. E. LUECKE, J. D. FRENCH, B. J. HOCKEY and S. M. WIEDERHORN, *J. Amer. Ceram. Soc.* **84** (1999) 1233.
18. F. LOFAJ, A. OKADA, Y. IKEDA, Y. MIZUTA, H. USAMI and H. KAWAMOTO, *Key Engineering Materials* **175/176** (2000) 321.
19. F. LOFAJ, A. OKADA, Y. IKEDA and H. KAWAMOTO, *ibid.* **171–174** (2000) 747.
20. F. LOFAJ, A. OKADA and H. KAWAMOTO, *J. Amer. Ceram. Soc.* **84** (1999) 1009.
21. ASTM E494-92a, "Standard practice for measuring ultrasonic velocity in materials," American society for testing and materials (West Conshohocken, PA, USA).
22. D. P. HURST and J. A. G. TEMPLE, *Int. J. Pres. Piping* **10** (1982) 451.
23. C. F. YING, in "Ultrasonic Measurement Method" (Academic Press, London, UK, 1990) p. 331.
24. J. TAKATSUBO and S. YAMAMOTO, *Nippon Kikai Gakkai Rombunshu* **A60** (1994) 2126 (in Japanese).
25. J. P. PANAKKAL, *IEEE Trans. on Ultrasonics* **38** (1991) 161.
26. N. KUMAR and J. P. PANAKKAL, *J. Mater. Sci.* **34** (1990) 4811.
27. K. K. PHANI and S. K. NIYOGI, *J. Mater. Sci. Lett.* **6** (1987) 511.
28. S. K. DATTA, A. K. MUKHOPADHYAY and D. CHAKRABORTY, *Am. Ceram. Soc. Bull.* **68** (1989) 2098.
29. W. A. FATE, *J. Amer. Ceram. Soc.* **57** (1974) 372.
30. M. KUPKOVA, *J. Mater. Sci.* **28** (1993) 5265.
31. A. R. BOCCACCINI and Z. FAN, *Ceramics International* **23** (1997) 239.

Received 4 January
and accepted 10 August 2000